

Investigations into the thermal non-equilibrium of W UMa-type contact binaries

Xiao Xiong, Liang Liu and Sheng-Bang Qian

Yunnan Observatories, Chinese Academy of Sciences, Kunming 650011, China; xiongx@ynao.ac.cn
Key Laboratory of the Structure and Evolution of Celestial Objects, Chinese Academy of Sciences, Kunming 650216, China

Center for Astronomical Mega-Science, Chinese Academy of Sciences, Beijing 100101, China
University of Chinese Academy of Sciences, Beijing 100049, China

Received 2018 January 16; accepted 2018 February 13

Abstract Traditionally, some physical details (e.g., magnetic braking, energy transfer, angular momentum loss, etc.) have to be taken into consideration during investigations into the evolution of contact binaries. However, the real evolutionary processes which usually contain several of these physical mechanisms are very complicated as a result of strong interaction between components. To avoid dealing with these factors, a linear relationship is applied to the temperatures of components. It is found that the higher the mass ratio (M_2/M_1) of a contact system, the weaker the deviation from thermal equilibrium. On this basis, a variation trend of fill-out factor (f) changing with mass ratio can be inferred, which is consistent with observations. Moreover, if we stick to this point of view, it should be natural that the number of semi-detached binaries in the predicted broken-contact phase of relaxation oscillations is less than the number in the contact phase.

Key words: stars: binaries: close — stars: binaries: eclipsing — stars: evolution

1 INTRODUCTION

According to Binnendijk (1970), W UMa-type contact binaries are divided into two subtypes: A and W. In this system of classification, temperatures of primaries are higher in A types and lower in W types than secondaries. Based on the investigations into period changes of W UMa-type systems by Ruciński (1973), W types might be thermally unstable, which contradicts the common envelope model built on thermal equilibrium by Lucy (1968). Based on the possibility of thermal non-equilibrium, thermal relaxation oscillation (TRO) theory was set up by Lucy (1976), Flannery (1976) and Robertson & Eggleton (1977). In this theory, W UMa-type contact systems are obliged to undergo periodic thermal relaxation oscillations between a contact phase and a semidetached phase. Because timescales spent in these two phases are roughly equal, both of their numbers should also be the same. Although candidates of pre-

dicted semidetached binaries have been found by Lucy & Wilson (1979), prediction about their numbers still seems to be incompatible with observation, such that an absence of this kind of binary still exists (Paczynski et al. 2006; Pietrukowicz et al. 2013). A possible explanation related to this contradiction refers to angular momentum loss considered by Li et al. (2005). Their model has the ability to undergo cycles without loss of contact. However, the evolutionary track of fill-out factor f versus mass ratio q is not consistent with observational facts.

On the basis of observations, many inferences about the evolutionary characteristics of W UMa-type contact binaries have been given by researchers. Based on the continuous transition of physical quantities and W types having a higher density in the primary than A types, there is the possibility of evolution from W types to A types after considering evolutionary expansion (Maceroni et al. 1985). From the view that statistical distributions of A types have higher average values than W types in both

total mass and orbital angular momentum, there is also the possibility of evolution from A types to W types when the loss of mass and angular momentum is taken into account (Gazeas & Niarchos 2006). Although the detailed mechanism is still a controversial problem, a contact system almost certainly cannot exist in a state of static equilibrium undergoing periodic thermal relaxation oscillations. Wang (1994) proposed that A types and W types are slowly expanding toward their equilibrium configuration and shrinking toward their zero age main sequence (ZAMS) point, and W types are caused by the gravitational energy released from contraction of the secondary which makes its effective temperature slightly higher than the primary. However, in the model of Li *et al.* (2004), contraction of the secondary is one of the mechanisms which leads to the appearance of W types. It only lasts for a very short period, so effective temperature of the secondary being higher than the primary is mainly caused by depletion of part of the luminosity of the primary due to its rapid expansion. In cyclic evolution, thermal equilibrium is unlikely to be achieved between components of a contact binary as a result of the difference in their thermal timescales. However, they still attempt to reach the non-existent case of thermal equilibrium, which is the driving force for the cyclic behavior.

From the above standpoints, it is clear that deviation from thermal equilibrium of a contact system leads to expansion or contraction of components and the expansion-contraction phenomenon is related to the interconversions between A types and W types. Owing to the difficulty of directly studying thermal non-equilibrium, the key aspect becomes interconversions between these two types, which can be considered as a natural laboratory for this kind of investigation. This paper investigates a variation trend in the degree of deviation from thermal equilibrium in cyclic evolution and constructs the relation between this evolutionary characteristic and observational data. Note that our topic in this paper is about thermal non-equilibrium of the whole contact system, not the transferred energy between components.

2 EVOLUTION UNDER LINEAR APPROXIMATION

2.1 Static Characteristics in Cyclic Evolution

Considering a real contact system in thermal non-equilibrium, the evolutionary track should always oscillate around thermal equilibrium, which cannot be reached. Hence, temperatures of two components (T_1 –

the primary; T_2 – the secondary) should also have similar oscillations near the isothermal state ($T_1 = T_2$), which corresponds to interconversions between A types and W types. As shown in Figure 1, this behavior is described by the solid line with label 2. In order to show the difference between thermal non-equilibrium and thermal equilibrium, it is assumed that there is another contact system in the non-existent case of thermal equilibrium. Hence, temperatures of components should always stay the same. This evolutionary behavior is associated with the straight solid line on the diagonal with label 1. Now, the difference between these two states is clear to us. The solid line 2 can be regarded as a spring. When a contact system in thermal non-equilibrium (line 2) gets closer to thermal equilibrium (line 1), the spring (line 2) has to be stretched. If the spring (line 2) is straightened, line 2 will be equivalent to line 1, which means that the contact system achieves thermal equilibrium, although this is impossible. Here, a state closer to thermal equilibrium than line 2 is introduced by the dashed line with label 3. In other words, the evolution track on line 3 is still in thermal non-equilibrium, but the degree of deviation from thermal equilibrium is weaker than for line 2. Additional information about Figure 1 is that the spring (line 2 or line 3) does not correspond to a real evolutionary track for a contact system in thermal non-equilibrium, but it is an approximation when a contact system enters into a state with a small temperature difference between its two components.

Accordingly, investigation into the degree of deviation from thermal equilibrium of a contact system depends on the differences between line 2 and line 3. Firstly, an imaginary point is placed in the lower right corner of Figure 1. This point is introduced and defined in the next subsection. Then we draw rays from this point and make them cover these two lines. Here, the slope of these rays is described by λ and temperature at intersections between line 2 or line 3 and the diagonal is represented by T_0 . Therefore, two differences are apparent to us:

- (1) The range of λ on line 3 is larger than that on line 2, which means that $\sigma(\lambda_3) > \sigma(\lambda_2)$. σ represents the standard deviation.
- (2) The interval between T_0 for two adjacent intersections on line 3 is also larger than that on line 2, which means that $\delta(T_{03}) > \delta(T_{02})$. δ represents the average of the interval.

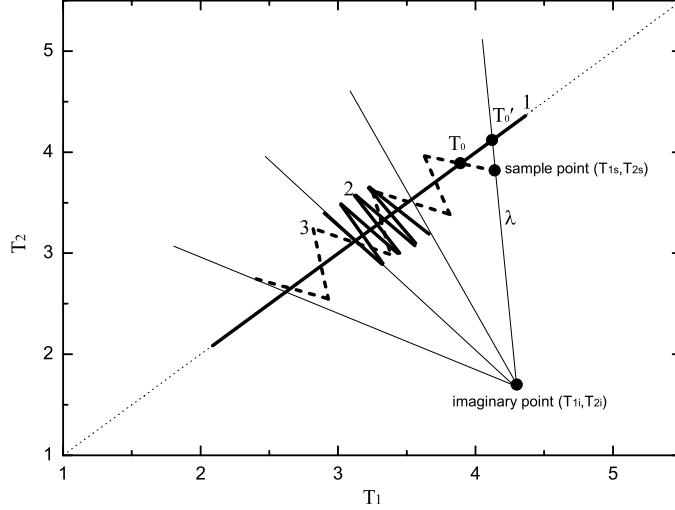


Fig. 1 Imaginary oscillations of temperatures around the isothermal state. The *straight solid line* on the diagonal with label 1 represents a contact system in the non-existent case of thermal equilibrium. The *solid line* with label 2 represents a contact system in thermal non-equilibrium. The *dashed line* with label 3 represents a contact system closer to thermal equilibrium than the *solid line* but still in thermal non-equilibrium. λ represents the slopes of the rays from the imaginary point. T_0 represents the intersections between line 2 or line 3 and the diagonal (*dotted line*). T_0' represents the intersections between these rays and the diagonal. Note that scales of axes are not the real values of temperatures but rather their relative variation trends.

Overall, a weaker deviation from thermal equilibrium requires two conditions — a larger $\sigma(\lambda)$ and a larger $\delta(T_0)$.

2.2 Method and Calculations

Rays from the imaginary point are described as

$$\frac{T_1 + \lambda' T_2}{1 + \lambda'} = T_0', \quad (1)$$

where λ' is the weighted parameter and T_0' is the isothermal temperature when $T_1 = T_2$.

Through an appropriate transformation, T_2 can be rewritten as a function of T_1 (i.e., $T_2 = -T_1/\lambda' + (1 + 1/\lambda')T_0'$). Then we have $\lambda = -1/\lambda'$. Hence, the comparison of $\sigma(\lambda)$ is equivalent to the comparison of $\sigma(\lambda')$. However, there is no correlation between T_0 and T_0' . As shown in Figure 1, the former comes from intersections between spring and diagonal, but the latter is from intersections between rays and diagonal. Fortunately, these rays also go through the spring, and the intersections between them represent samples of W UMA-type contact binaries consisting of A types and W types. If the samples are random enough, the comparison of $\delta(T_0)$ will also be equivalent to the comparison of $\delta(T_0')$. Here, 118 samples of W UMA-type contact binaries with sufficient absolute quantities (e.g., mass, radius, luminosity, etc.)

have been collected. They are listed in Table 1 (A types) and Table 2 (W types), and we presuppose that these samples are random. Hence, two original conditions on $\sigma(\lambda)$ and $\delta(T_0)$ are converted into conditions on $\sigma(\lambda')$ and $\delta(T_0')$.

Let us come back to Equation (1). There are two points on each of the rays. One point is from the samples on the spring. The other is the imaginary point which is still unknown to us. Hence, a unified definition of this point is needed. In this paper, this imaginary point is set in the critical phase between the contact phase and the broken-contact phase for convenience, which means that the fill-out factor of a contact system on this point should be equal to 0 and the transferred energy between components is at a low level because of the poor thermal contact. Owing to the mass difference, the secondary (the less massive one) should be more sensitive to the transferred energy than the primary (the more massive one). Based on these restrictions and the fact that components of most EWs are main sequence (MS) stars (Qian et al. 2017), luminosities of the two components at the imaginary point are roughly equal to those on the MS, and the MS radius of the primary is maintained. However, radius of the secondary has to be computed by Roche geometry. Accordingly, temperatures of a contact system at the

Table 1 Samples of A-type Contact Binaries

Star	Per (d)	M_1 (M_\odot)	M_2 (M_\odot)	R_1 (R_\odot)	R_2 (R_\odot)	L_1 (L_\odot)	L_2 (L_\odot)	T_1 (K)	T_2 (K)	q_{ph}	f	Reference	λ'	T_0' (T_\odot)
CC Com	0.2207	0.720	0.379	0.708	0.522	0.151	0.079	4300	4263	0.529	0.180	Zola et al. (2010)	1.00979	0.74073
J1558	0.2601	1.300	0.800	0.940	0.770	1.170	0.675	6200	5970	0.650	0.069	Djurašević et al. (2016)	1.14952	1.05138
VZ Psc	0.2613	0.560	0.510	0.660	0.650	0.160	0.130	4500	4305	0.920	0.070	Maceroni et al. (1990)	-1.08343	0.34041
VW Cep	0.2783	0.851	0.340	0.870	0.568	1.246	0.373	6547	5993	0.401	0.180	Khajavi et al. (2002)	-0.18466	1.15441
XY Leo	0.2841	0.813	0.593	0.833	0.714	0.448	0.220	5200	4701	0.717	0.080	Zola et al. (2010)	0.53315	0.86963
TZ Boo	0.2972	0.990	0.210	1.080	0.560	1.260	0.330	5890	5873	0.207	0.525	Christopoulou et al. (2011)	0.11748	1.01872
SX Crv	0.3166	1.246	0.098	1.347	0.409	2.627	0.216	6340	6160	0.079	0.270	Zola et al. (2004)	0.12572	1.09341
ASAS 0212	0.3182	1.150	0.220	1.180	0.580	0.990	0.230	5307	5254	0.189	0.587	Acerbi et al. (2011)	0.45543	0.91530
AH Tau	0.3327	1.040	0.530	1.050	0.770	1.190	0.640	5840	5816	0.505	0.066	Xiang et al. (2015)	0.22795	1.00961
EQ Tau	0.3413	1.233	0.551	1.143	0.775	1.360	0.610	5860	5810	0.447	0.130	Zola et al. (2005)	0.38098	1.01145
V508 Oph	0.3448	1.010	0.520	1.060	0.800	1.305	0.662	6000	5830	0.530	0.104	Lapasset & Gomez (1990)	0.13863	1.03448
GR Vir	0.3470	1.370	0.170	1.420	0.610	2.870	0.480	6300	6163	0.122	0.786	Qian & Yang (2004)	0.20716	1.08590
CK Boo	0.3552	1.386	0.154	1.448	0.586	2.716	0.434	6380	6340	0.111	0.717	Yang et al. (2012)	0.18504	1.10273
AH Cnc	0.3605	1.188	0.185	1.332	0.592	2.504	0.449	6300	6151	0.156	0.510	Peng et al. (2016)	0.11903	1.08722
UCAC4	0.3615	0.700	0.300	1.000	0.650	0.398	0.167	4590	4580	0.400	0.077	Djurašević et al. (2016)	0.50464	0.79354
DZ Psc	0.3661	1.352	0.183	1.469	0.617	2.836	0.493	6210	6187	0.145	0.790	Gazeas et al. (2005)	0.22152	1.07367
V410 Aur	0.3663	1.304	0.188	1.397	0.605	2.294	0.396	6040	5915	0.143	0.524	Yang et al. (2005a)	0.25653	1.04057
XY Boo	0.3706	0.912	0.169	1.230	0.607	2.138	0.515	6324	6307	0.186	0.559	Yang et al. (2005a)	-0.04862	1.09427
U Peg	0.3748	1.149	0.379	1.224	0.744	1.583	0.577	5860	5841	0.331	0.244	Pribulla & Vanko (2002)	0.26957	1.01314
DX Tuc	0.3771	1.000	0.300	1.200	0.710	1.970	0.660	6250	6182	0.290	0.149	Szalai et al. (2007)	0.02606	1.08102
HN UMa	0.3825	1.279	0.179	1.435	0.583	2.550	0.410	6100	6082	0.147	0.320	Zola et al. (2005)	0.21662	1.05481
AU Ser	0.3865	0.895	0.635	1.100	0.940	0.988	0.541	5495	5114	0.710	0.198	Gürol (2005)	0.36036	0.93323
EX Leo	0.4086	1.573	0.313	1.560	0.734	3.474	0.663	6340	6110	0.200	0.350	Zola et al. (2010)	0.33173	1.08697
QX And	0.4122	1.470	0.450	1.460	0.880	3.285	1.179	6440	6420	0.306	0.352	Djurašević et al. (2011)	0.25860	1.11348
V1918 Cyg	0.4132	1.520	0.400	1.520	0.870	5.143	1.559	7060	6924	0.264	0.497	Yang et al. (2013)	0.09870	1.21934
RZ Tau	0.4157	1.700	0.640	1.560	1.040	6.190	2.600	7300	7194	0.379	0.550	Yang & Liu (2003b)	0.17146	1.26029
Y Sex	0.4198	1.210	0.220	1.500	0.750	3.000	0.690	6210	6093	0.180	0.640	Yang & Liu (2003a)	0.16040	1.07160
V899 Her	0.4212	2.100	1.190	1.570	1.220	2.320	1.400	5700	5677	0.566	0.237	Özdemir et al. (2002)	-4.75760	0.98112
AK Her	0.4215	1.200	0.340	1.400	0.800	3.020	0.820	6500	6180	0.277	0.332	Çalışkan et al. (2014)	0.08837	1.12007
EF Dra	0.4240	1.815	0.290	1.702	0.777	3.961	0.793	6250	6186	0.160	0.467	Yang (2012)	0.52228	1.07752
AW UMa	0.4387	1.636	0.162	1.752	0.656	6.530	0.570	6980	6201	0.099	0.353	Pribulla & Rucinski (2008)	0.16436	1.18859
DN Boo	0.4476	1.428	0.148	1.710	0.670	3.750	0.560	6095	6071	0.103	0.640	Şenavcı et al. (2008)	0.28103	1.05359
FO Hya	0.4696	1.310	0.310	1.620	0.910	5.650	0.550	7000	5213	0.238	0.680	Prasad et al. (2013)	0.02117	1.20466
DK Cyg	0.4707	1.741	0.533	1.708	0.986	8.270	1.755	7500	6700	0.306	0.300	Baran et al. (2004)	0.15900	1.27859
VW LMi	0.4776	1.680	0.710	1.690	1.180	4.402	1.820	6440	6180	0.423	0.504	Djurašević et al. (2013)	1.02014	1.09147
XZ Leo	0.4877	1.742	0.586	1.689	1.004	6.926	2.073	7240	6946	0.336	0.190	Gazeas et al. (2006)	0.22054	1.24340
OO Aql	0.5068	1.060	0.897	1.406	1.309	2.453	1.894	6100	5926	0.846	0.370	Li et al. (2016)	6.65555	1.02919
V357 Peg	0.5785	0.850	0.340	1.480	0.990	4.730	1.770	7000	6687	0.401	0.312	Ekmekçi et al. (2012)	-0.26847	1.23095
ε CrA	0.5914	1.700	0.230	2.100	0.850	7.750	1.020	6678	6341	0.128	0.252	Yang et al. (2005b)	0.30934	1.14159
V2150 Cyg	0.5919	2.350	1.885	1.982	1.786	14.416	11.245	8000	7920	0.802	0.190	Kreiner et al. (2003)	-3.47652	1.36465
AQ Tuc	0.5948	1.930	0.690	2.050	1.320	8.950	3.470	6982	6866	0.350	0.580	Hilditch & King (1986)	0.43678	1.20186
HI Dra	0.5974	1.700	0.420	1.970	1.070	7.870	1.800	7000	6550	0.250	0.230	Çalışkan et al. (2014)	0.25551	1.19523
V402 Aur	0.6035	1.638	0.327	1.997	0.915	7.528	1.512	6775	6700	0.200	0.030	Zola et al. (2004)	0.21591	1.16984
RR Cen	0.6057	1.820	0.380	2.100	1.050	8.890	2.200	6912	6891	0.205	0.351	Yang et al. (2005b)	0.31986	1.19497
UZ Leo	0.6181	1.989	0.603	2.286	1.389	10.964	3.708	6980	6830	0.309	0.970	Zola et al. (2010)	0.45972	1.19944
FP Boo	0.6405	1.604	0.154	2.310	0.774	11.193	0.920	6980	6456	0.096	0.380	Gazeas et al. (2006)	0.14171	1.19636
IK Per	0.6760	1.990	0.340	2.400	1.150	35.040	5.670	9070	8597	0.171	0.600	Zhu et al. (2005)	-0.05568	1.57403
HV UMa	0.7108	2.800	0.500	2.620	1.180	15.400	2.900	7074	6944	0.184	0.018	Csák et al. (2000)	0.83013	1.21367
V592 Per	0.7157	1.743	0.678	2.252	1.468	9.580	2.500	6800	6020	0.389	0.590	Zola et al. (2005)	0.46449	1.13367
V1073 Cyg	0.7859	1.730	0.530	2.330	1.360	9.770	3.010	6700	6520	0.303	0.174	Ekmekçi et al. (2012)	0.38035	1.15059
V376 And	0.7987	2.491	0.759	2.662	1.549	30.441	6.139	8350	7335	0.320	0.240	Zola et al. (2010)	0.60400	1.37851
V2388 Oph	0.8023	1.800	0.340	2.600	1.300	13.500	2.430	6900	6349	0.186	0.650	Yakut et al. (2004)	0.34528	1.16930
TY Pup	0.8193	2.300	0.420	2.840	1.390	26.915	5.754	7800	7567	0.185	0.520	Gu et al. (1993)	0.33374	1.33939
V921 Her	0.8774	2.068	0.505	2.752	1.407	23.526	5.094	7700	7346	0.244	0.230	Gazeas et al. (2006)	0.26846	1.31922
DU Boo	1.0559	2.080	0.487	3.190	1.740	34.622	9.098	7850	7610	0.234	0.502	Djurašević et al. (2013)	0.22633	1.35047

Table 3 Calculation Results for $\sigma(\lambda')$ and $\delta(T_0')$

q	$\sigma(\lambda')$	$\delta(T_0')$
0.0 – 0.1 (0.05)	0.10282	0.05564
0.1 – 0.2 (0.15)	0.18334	0.02994
0.2 – 0.3 (0.25)	0.15015	0.01474
0.3 – 0.4 (0.35)	0.20294	0.02005
0.4 – 0.5 (0.45)	0.36887	0.02508
0.5 – 0.6 (0.55)	1.91961	0.04142
0.6 – 0.7 (0.65)	1.13679	0.11149
0.7 – 0.8 (0.75)	7.16099	0.04629
0.8 – 1.0 (0.90)	7.59619	0.34141

imaginary point can be written as

$$(T_{1i}, T_{2i}) = \left(\left(\frac{L_{1i}}{R_{1i}^2} \right)^{0.25}, \left(\frac{L_{2i}}{r_{21}^2 R_{1i}^2} \right)^{0.25} \right), \quad (2)$$

where T_{1i} and T_{2i} represent temperatures of the primary and secondary at the imaginary point respectively, L_{1i} and L_{2i} are their luminosities on the MS, R_{1i} is MS radius of the primary and r_{21} represents the radius ratio of the secondary to the primary. Calculation of r_{21} refers to the method proposed by Liu *et al.* (2018). About the calculations of L_i and R_i , formulae describing the mass-luminosity relation and mass-radius relation for MS stars from Demircan & Kahraman (1991) are adopted

$$L_i \cong \begin{cases} 0.20M^{2.50} & M < 0.7 M_{\odot} \\ 1.15M^{3.36} & M > 0.7 M_{\odot}, \end{cases} \quad (3)$$

$$R_i \cong \begin{cases} 0.89M^{0.89} & M < 1.66 M_{\odot} \\ 1.01M^{0.57} & M > 1.66 M_{\odot}. \end{cases} \quad (4)$$

So far, two sets of temperatures, (T_{1i}, T_{2i}) and (T_{1s}, T_{2s}) , are known to us. (T_{1i}, T_{2i}) is from the imaginary point and (T_{1s}, T_{2s}) from the samples on the spring. Hence, calculations of λ' and T_0' can be carried out by Equation (1). Values of these two quantities associated with each of the samples are listed in the last two columns of Table 1 and Table 2. Additionally, we also plot them in Figure 2 and Figure 3. Both of their abscissas represent the mass ratio of sample systems. In order to compute $\sigma(\lambda')$ and $\delta(T_0')$, interval division of mass ratio is needed. Here, the range from 0 to 1 is divided into 10 intervals of 0.1. The last interval $[0.9, 1]$ merges with $[0.8, 0.9]$ into a larger one representing $[0.8, 1]$, because there is only one sample in it. Calculation results for $\sigma(\lambda')$ and $\delta(T_0')$ are shown in Table 3 and are drawn in Figure 4 and Figure 5 respectively. It is clear that both $\sigma(\lambda')$ and $\delta(T_0')$ have a trend to be larger and larger with the increase of mass ratio, roughly. Hence, we can draw a conclusion that the higher the mass ratio (M_2/M_1) of

a contact system, the weaker the deviation from thermal equilibrium.

3 EVIDENCE IN OBSERVATIONS

Considering a contact system in thermal non-equilibrium, energy transfer from the primary to the secondary happens because of overluminosity of the latter (Yang & Liu 2001) and the approximate equality between the sum of surface luminosities of components and the sum of their nuclear luminosities (Jiang *et al.* 2009). Unfortunately, transferred energy between components has nothing to do with energy sources and sinks. It is just a process happening inside a contact system, which is not associated with thermal non-equilibrium of the whole system. In order to make the thermal non-equilibrium clear, an equation describing energy conservation is needed

$$L_{1nuc} + L_{2nuc} = L_{1sur} + L_{2sur} + \Delta(L), \quad (5)$$

where L_{1nuc} and L_{2nuc} are the nuclear luminosities of the primary and the secondary respectively, L_{1sur} and L_{2sur} are their surface luminosities, and $\Delta(L)$ represents the variation in gravitational potential of the contact system with a small magnitude because of the fact of approximate equality found by Jiang *et al.* (2009).

When $\Delta(L) = 0$, energy generated from nuclear reactions is equal to energy released from the system's surface, which means the contact system is in thermal equilibrium. On the contrary, when $\Delta(L) \neq 0$, energy generated from nuclear reactions is unequal to energy released from the system's surface, which means the contact system is in thermal non-equilibrium. Hence, $\Delta(L)$ (variation in gravitational potential) is directly related to the deviation from thermal equilibrium. Because $\Delta(L)$ corresponds to the phenomenon of expansion and contraction, deviation from thermal equilibrium causes expansion or contraction of components.

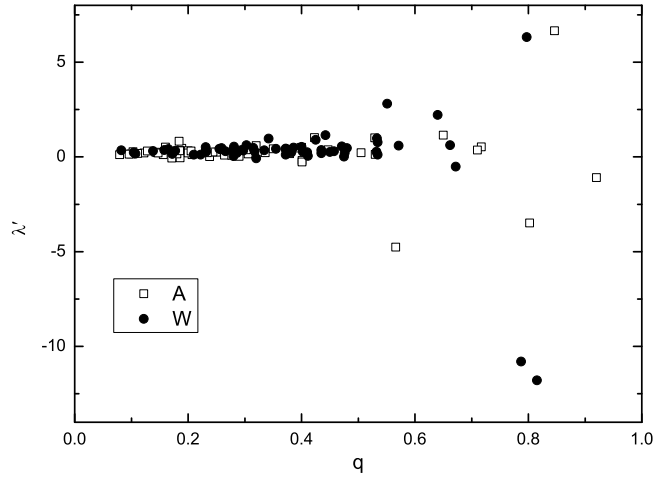


Fig. 2 Distribution of the weighted parameter λ' versus mass ratio q . *White squares* represent samples from A types. *Black circles* represent samples from W types.

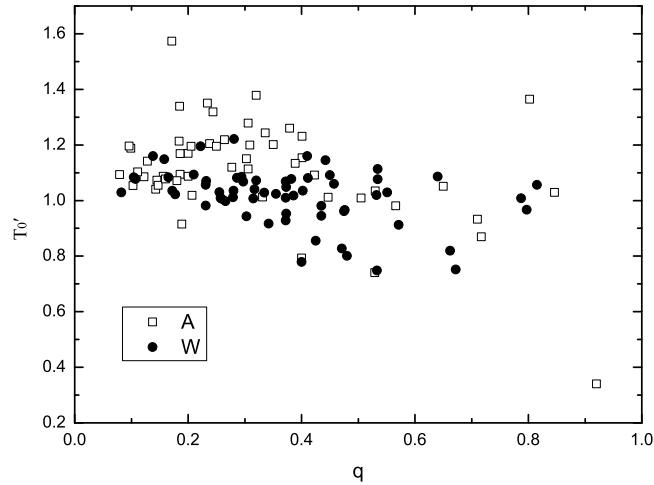


Fig. 3 Distribution of the isothermal temperature T_0' versus mass ratio q . *White squares* represent samples from A types. *Black circles* represent samples from W types.

Accordingly, the expansion-contraction phenomenon resulting from thermal non-equilibrium appears on the primary or the secondary, which leads to matter entering or leaving the common envelope. Additionally, the fill-out factor f can be regarded as an indicator for thickness of the common envelope. Behavior of the common envelope is predictable in that there should be a greater amplitude on the fill-out factor (i.e., $\Delta(f)$), when the degree of deviation from thermal equilibrium becomes larger (which means a greater $\Delta(L)$). Combined with the conclusion that a higher mass ratio is related to a weaker deviation from thermal equilibrium, it is natural that the smaller the mass

ratio, the larger the fill-out factor distribution range. Distribution of f versus q for our samples is presented in Figure 6. It is in line with our expectation. We also make a comparison with figure 4 in Liu et al. (2018). Most of their samples are from Yakut & Eggleton (2005). It shows a similar distribution of f except for two interesting targets, NSVS 925605 (Dimitrov & Kjurkchieva 2015) and 1SWASP J075102.16+342405.3 (Jiang et al. 2015). They seem to contradict our opinion about the deviation from thermal equilibrium because of their high mass ratios and large fill-out factors. Here, we propose a conjecture that these two rare samples might be in a special evolutionary stage if their solutions are

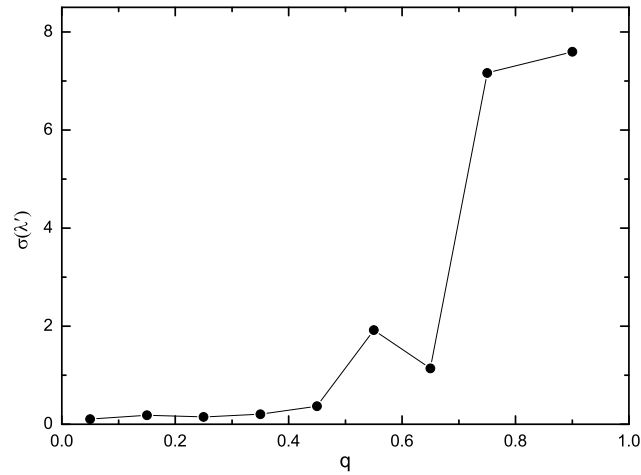


Fig. 4 Relation between standard deviation of weighted parameter $\sigma(\lambda')$ and mass ratio q .

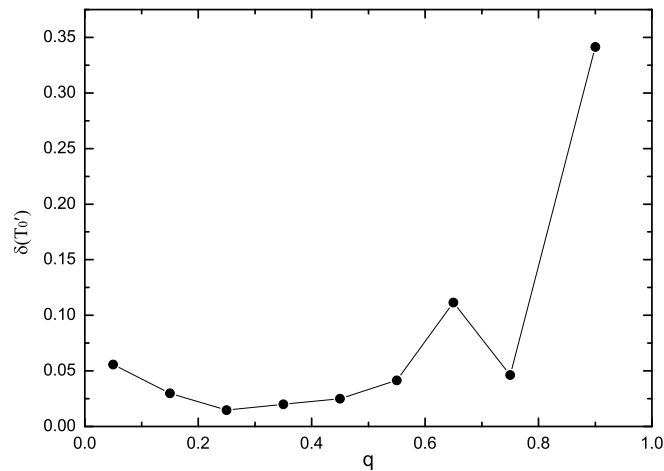


Fig. 5 Relation between average interval of isothermal temperature $\delta(T_0')$ and mass ratio q .

reliable. The most probable cause is that one of their components has evolved into post-MS. However, it is not easy to identify the evolution state from spectral observations as a result of mass transfer.

When a contact system has achieved the non-existent case of thermal equilibrium, there is no need for oscillations between the contact phase and the broken-contact phase owing to $\Delta(L) = 0$, which means gravitational potential stays stable and no expansion-contraction phenomenon happens. Under the same logic, a real contact system in thermal non-equilibrium might not enter into the predicted broken-contact phase if the degree of deviation from thermal equilibrium is small enough. Based on the discovery of a higher mass ratio corresponding to a weaker deviation from thermal equilib-

rium, contact systems with high mass ratios should have the ability to avoid the broken-contact phase. As a result, both of their numbers are different from each other. The number of the latter (in the broken-contact phase) could be much less than that of the former (in the contact phase) when the mass ratio is large enough. In fact, there is a large difference in their numbers (Paczyński *et al.* 2006; Pietrukowicz *et al.* 2013), which is consistent with our expectation. Although these statistical analyses are based upon the period, their samples should be distributed in the whole range of mass ratio. However, further research that involves statistical analysis based on mass ratio is still needed to verify this expectation. Note that the evolutionary track of f versus q in figure 6(a) of Li *et al.* (2005) does not fit with the observational facts

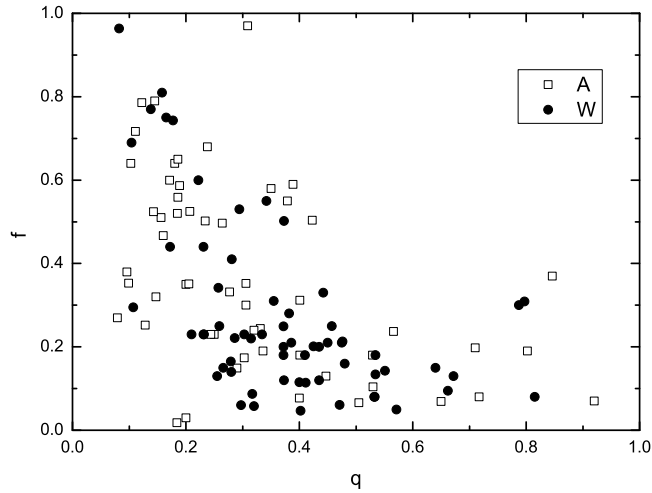


Fig. 6 Distribution of fill-out factor f versus mass ratio q . *White squares* represent samples from A types. *Black circles* represent samples from W types.

in Figure 6, even though their model can be prevented from the broken-contact phase after considering angular momentum loss due to magnetic stellar wind.

4 DISCUSSIONS AND CONCLUSIONS

The limitation of this paper rests with samples we have collected, which are thought to be random enough. About the imaginary point in Figure 1, maybe the calculations are not in accordance with physical reality, but this aspect does not matter. We only focus on a unified definition of this point for all the samples. The key in this paper is linear Equation (1) we have introduced. It is very concise, so lots of physical mechanisms can be avoided. There is a slight difference in values of λ' and T_0' when the empirical formulae for MS cases (i.e., Eq. (3) and Eq. (4)) change, but the distributions of $\sigma(\lambda')$ and $\delta(T_0')$ in Figure 4 and Figure 5 still remain similar. Accordingly, conclusions about the evolution characteristics of W UMA-type contact binaries are reliable:

- (1) Degree of deviation from thermal equilibrium of a contact system decreases with the increase in its mass ratio.
- (2) The fill-out factor distribution range becomes larger as the mass ratio becomes smaller (in accordance with observations).
- (3) A contact system with a high mass ratio should have the ability to avoid the broken-contact phase because of a weak deviation from thermal equilibrium (in accordance with observations, but further investigation is still needed).

Acknowledgements This work is partly supported by the Yunnan Natural Science Foundation (2016FB004), the Young Academic and Technology Leaders project of Yunnan Province (No. 2015HB098), the National Natural Science Foundation of China (Nos. 11773066, 11403095 and 11325315) and the Key Research Programme of the Chinese Academy of Sciences (Grant No. KGZD-EW-603).

References

- Acerbi, F., Barani, C., & Martignoni, M. 2011, RAA (Research in Astronomy and Astrophysics), 11, 843
- Albayrak, B., Djurašević, G., Erkapic, S., & Tanriverdi, T. 2004, A&A, 420, 1039
- Alvarez, G. E., Sowell, J. R., Williamon, R. M., & Lapasset, E. 2015, PASP, 127, 742
- Baran, A., Zola, S., Rucinski, S. M., et al. 2004, Acta Astronomica, 54, 195
- Barone, F., di Fiore, L., Milano, L., & Russo, G. 1993, ApJ, 407, 237
- Binnendijk, L. 1970, Vistas in Astronomy, 12, 217
- Çalışkan, Ş., Latković, O., Djurašević, G., et al. 2014, AJ, 148, 126
- Christopoulou, P.-E., & Papageorgiou, A. 2013, AJ, 146, 157
- Christopoulou, P.-E., Papageorgiou, A., & Chrysopoulos, I. 2011, AJ, 142, 99
- Csák, B., Kiss, L. L., Vinkó, J., & Alfaro, E. J. 2000, A&A, 356, 603
- Demircan, O., & Kahraman, G. 1991, Ap&SS, 181, 313
- Dimitrov, D. P., & Kjurkchieva, D. P. 2015, MNRAS, 448, 2890

- Djurašević, G., Essam, A., Latković, O., et al. 2016, *AJ*, 152, 57
- Djurašević, G., Yılmaz, M., Baştürk, Ö., et al. 2011, *A&A*, 525, A66
- Djurašević, G., Baştürk, Ö., Latković, O., et al. 2013, *AJ*, 145, 80
- Ekmekçi, F., Elmaslı, A., Yılmaz, M., et al. 2012, *New Astron.*, 17, 603
- Erdem, A., & Özkardeş, B. 2009, *New Astron.*, 14, 321
- Erkan, N., & Ulaş, B. 2016, *New Astron.*, 46, 73
- Flannery, B. P. 1976, *ApJ*, 205, 217
- Gazeas, K. D., & Niarchos, P. G. 2006, *MNRAS*, 370, L29
- Gazeas, K. D., Niarchos, P. G., Zola, S., Kreiner, J. M., & Rucinski, S. M. 2006, *Acta Astronomica*, 56, 127
- Gazeas, K. D., Baran, A., Niarchos, P., et al. 2005, *Acta Astronomica*, 55, 123
- Goecking, K.-D., Duerbeck, H. W., Plewa, T., et al. 1994, *A&A*, 289, 827
- Gu, S., Yang, Y., Liu, Q., & Zhang, Z. 1993, *Ap&SS*, 203, 161
- Gürol, B. 2005, *New Astron.*, 10, 653
- He, J.-J., & Qian, S.-B. 2008, *ChJAA (Chin. J. Astron. Astrophys.)*, 8, 465
- Hilditch, R. W., Hill, G., & Bell, S. A. 1992, *MNRAS*, 255, 285
- Hilditch, R. W., & King, D. J. 1986, *MNRAS*, 223, 581
- Jiang, D., Han, Z., Jiang, T., & Li, L. 2009, *MNRAS*, 396, 2176
- Jiang, L., Qian, S.-B., Zhang, J., & Liu, N. 2015, *PASJ*, 67, 118
- Kaluzny, J., & Rucinski, S. M. 1986, *AJ*, 92, 666
- Khajavi, M., Edalati, M. T., & Jassur, D. M. Z. 2002, *Ap&SS*, 282, 645
- Kreiner, J. M., Rucinski, S. M., Zola, S., et al. 2003, *A&A*, 412, 465
- Lapasset, E., & Gomez, M. 1990, *A&A*, 231, 365
- Lee, J. W., Lee, C.-U., Kim, S.-L., Kim, H.-I., & Park, J.-H. 2011, *PASP*, 123, 34
- Li, H.-L., Wei, J.-Y., Yang, Y.-G., & Dai, H.-F. 2016, *RAA (Research in Astronomy and Astrophysics)*, 16, 2
- Li, L., Han, Z., & Zhang, F. 2004, *MNRAS*, 351, 137
- Li, L., Han, Z., & Zhang, F. 2005, *MNRAS*, 360, 272
- Liao, W.-P., Qian, S.-B., Li, K., et al. 2013, *AJ*, 146, 79
- Liu, L., Qian, S.-B., & Xiong, X. 2018, *MNRAS*, 474, 5199
- Lu, W.-X., & Rucinski, S. M. 1993, *AJ*, 106, 361
- Lucy, L. B. 1968, *ApJ*, 153, 877
- Lucy, L. B. 1976, *ApJ*, 205, 208
- Lucy, L. B., & Wilson, R. E. 1979, *ApJ*, 231, 502
- Maceroni, C., Milano, L., & Russo, G. 1985, *MNRAS*, 217, 843
- Maceroni, C., van Hamme, W., & van't Veer, F. 1990, *A&A*, 234, 177
- Özdemir, S., Demircan, O., Erdem, A., et al. 2002, *A&A*, 387, 240
- Paczyński, B., Szczygieł, D. M., Pilecki, B., & Pojmański, G. 2006, *MNRAS*, 368, 1311
- Peng, Y.-J., Luo, Z.-Q., Zhang, X.-B., et al. 2016, *RAA (Research in Astronomy and Astrophysics)*, 16, 157
- Pietrukowicz, P., Mróz, P., Soszyński, I., et al. 2013, *Acta Astronomica*, 63, 115
- Prasad, V., Pandey, J. C., Patel, M. K., & Srivastava, D. C. 2013, *New Astron.*, 20, 52
- Pribulla, T., & Rucinski, S. M. 2008, *MNRAS*, 386, 377
- Pribulla, T., & Vanko, M. 2002, *Contributions of the Astronomical Observatory Skalnaté Pleso*, 32, 79
- Qian, S.-B., He, J.-J., Liu, L., Zhu, L.-Y., & Liao, W. P. 2008, *AJ*, 136, 2493
- Qian, S.-B., He, J.-J., Zhang, J., et al. 2017, *RAA (Research in Astronomy and Astrophysics)*, 17, 087
- Qian, S.-B., & Yang, Y.-G. 2004, *AJ*, 128, 2430
- Qian, S.-B., Yang, Y.-G., Soonthornthum, B., et al. 2005, *AJ*, 130, 224
- Qian, S.-B., Yuan, J.-Z., Xiang, F.-Y., et al. 2007, *AJ*, 134, 1769
- Robertson, J. A., & Eggleton, P. P. 1977, *MNRAS*, 179, 359
- Ruciński, S. M. 1973, *Acta Astronomica*, 23, 79
- Samec, R. G., & Hube, D. P. 1991, *AJ*, 102, 1171
- Şenavcı, H. V., Nelson, R. H., Özavcı, İ., Selam, S. O., & Albayrak, B. 2008, *New Astron.*, 13, 468
- Szalai, T., Kiss, L. L., Mészáros, S., Vinkó, J., & Csizmadia, S. 2007, *A&A*, 465, 943
- Wang, J.-M. 1994, *ApJ*, 434, 277
- Xiang, F.-Y., Xiao, T.-Y., & Yu, Y.-X. 2015, *AJ*, 150, 25
- Yakut, K., & Eggleton, P. P. 2005, *ApJ*, 629, 1055
- Yakut, K., Kalomeni, B., & İbanoğlu, C. 2004, *A&A*, 417, 725
- Yang, Y.-G. 2012, *RAA (Research in Astronomy and Astrophysics)*, 12, 419
- Yang, Y.-G., Qian, S.-B., & Zhu, C.-H. 2004, *PASP*, 116, 826
- Yang, Y.-G., Qian, S.-B., & Zhu, L.-Y. 2005a, *AJ*, 130, 2252
- Yang, Y.-G., Qian, S.-B., Zhu, L.-Y., He, J.-J., & Yuan, J.-Z. 2005b, *PASJ*, 57, 983
- Yang, Y.-G., Qian, S.-B., & Soonthornthum, B. 2012, *AJ*, 143, 122
- Yang, Y.-G., Qian, S.-B., & Dai, H.-F. 2013, *AJ*, 145, 60
- Yang, Y., & Liu, Q. 2001, *AJ*, 122, 425
- Yang, Y., & Liu, Q. 2003a, *New Astron.*, 8, 465
- Yang, Y., & Liu, Q. 2003b, *AJ*, 126, 1960
- Zhang, X. B., Deng, L., & Lu, P. 2009, *AJ*, 138, 680
- Zhu, L.-Y., Qian, S.-B., Soonthornthum, B., & Yang, Y.-G. 2005, *AJ*, 129, 2806
- Zola, S., Gazeas, K., Kreiner, J. M., et al. 2010, *MNRAS*, 408, 464
- Zola, S., Niarchos, P., Manimanis, V., & Dapergolas, A. 2001, *A&A*, 374, 164
- Zola, S., Rucinski, S. M., Baran, A., et al. 2004, *Acta Astronomica*, 54, 299
- Zola, S., Kreiner, J. M., Zakrzewski, B., et al. 2005, *Acta Astronomica*, 55, 389